Changes to environmental parameters that control tropical cyclone genesis under global warming

Hiroyuki Murakami,[1] Tim Li,[2,3] and Melinda Peng[4]

Received 26 February 2013; revised 20 March 2013; accepted 21 March 2013.

[1] This study uses the Meteorological Research Institute high-resolution Atmospheric Climate Model to determine whether environmental parameters that control tropical cyclone genesis in the Western North Pacific (WNP) and North Atlantic (NA) may differ in the global warming state. A box difference index was computed to quantitatively assess the role of environmental controlling parameters. The diagnosis of the model outputs shows that in the WNP, dynamic variables are of primary importance for separating developing and nondeveloping disturbances in the present-day climate, and such a relationship remains unchanged in a future warmer climate. This is in contrast to the NA, where box difference index increases for all dynamic variables investigated while it shows little change for thermodynamic variables. This implies that, when compared with the present-day climate in which thermodynamic variables have a major control on tropical cyclone genesis, dynamic and thermodynamic variables have equal control in the NA under the future warmer climate. **Citation:** Murakami, H., T. Li, and M. Peng (2013), Changes to environmental parameters that control tropical cyclone genesis under global warming, *Geophys. Res. Lett.*, *40*, doi:10.1002/grl.50393.

1. Introduction

[2] A number of studies have used state-of-the-art climate models to assess possible future changes in the frequency of tropical cyclone (TC) genesis under global warming [e.g., *Knutson et al*., 2010]. To understand mechanisms linked to changes in TC genesis frequency, a number of large-scale dynamic and thermodynamic parameters have been identified [e.g., *Li et al*., 2010; *Lavender and Walsh*, 2011; *Murakami et al*., 2012a,b; *Zhao and Held*, 2012; *Li*, 2012]. Some studies also used a genesis potential index (GPI) [*Emanuel and Nolan*, 2004] to identify the relative importance of large-scale variables on projected future changes in the TC genesis frequency [e.g., *Vecchi and Soden*, 2007; *Yokoi and Takayabu*, 2009; *Murakami et al*., 2011]. However, these studies assumed that the same set of large-scale variables or parameters that control the present-day (PD) TC genesis will also control future TC genesis. An open question remains: Will the large-scale controlling variables for TC genesis be different under a future warmer climate? *Nolan and Rappin* [2008] found that vertical wind shear is more effective in suppressing TC genesis when the sea surface temperature (SST) is higher. This implies that the relative importance of large-scale dynamic and thermodynamic conditions favorable (or unfavorable) for TC genesis may change as the climate state of the Earth changes in the future.

[3] In this study, we analyze climate simulations using a box difference index (BDI) [*Peng et al*., 2012; *Fu et al*., 2012] to quantitatively assess the environmental controlling parameters for TC genesis in the tropical western North Pacific (WNP) and North Atlantic (NA). As will be explained in section 2, the BDI is a useful tool to identify the relative importance of large-scale variables that are most effective in separating environments favorable for developing disturbances from those that do not. *Peng et al*. [2012] suggest from observations that thermodynamic variables are of primary importance for the separation of developing disturbances from nondeveloping disturbances in the NA, while dynamic parameters are of primary importance in the WNP [*Fu et al*., 2012]. This study aimed to address two questions: Can a high-resolution atmospheric climate model reproduce the observed basin contrast in prevailing large-scale controlling parameters described above? Will the prevailing large-scale variables change as the climate warms in the future? The remainder of this paper is organized as follows. Section 2 provides a description of the experimental design and analysis strategy. Section 3 presents the results and discussion. Finally, a summary is given in section 4.

2. Methods

2.1. Model and Simulation Settings

[4] The climate simulations were conducted using the high-resolution 20 km mesh Meteorological Research Institute (MRI) Atmospheric General Circulation Model (AGCM) version 3.2 (MRI-AGCM3.2) [*Mizuta et al*., 2012]. Two experiments are designed: the first one is for the present-day period (1979–2003) and the second one is for the future warmer climate state (2075–2099). The simulation configurations are the same as those described in *Murakami et al*. [2012a]. In short, the so-called time-slice method [*Bengtsson et al*., 1996] was applied, in which the high-resolution AGCM is forced by setting the lower boundary conditions to a prescribed SST and sea ice concentration (SIC). The PD

Additional supporting information may be found in the online version of this article.

[1]International Pacific Research Center, University of Hawaii at Manoa, Honolulu, Hawaii, 96822, USA.
[2]Department of Meteorology and International Pacific Research Center, University of Hawaii at Manoa, Honolulu, Hawaii, 96822, USA.
[3]Also at Key Laboratory of Meteorological Disaster, College of Atmospheric Science, Nanjing University of Information Science and Technology, Nanjing, China.
[4]Naval Research Laboratory, Monterey, California, 93943, USA.

Corresponding author: T. Li, Department of Meteorology and International Pacific Research Center, University of Hawaii at Manoa, Honolulu, HI 96822, USA. (timli@hawaii.edu)

0094-8276/13/10.1002/grl.50393

experiment for the period 1979–2003 can be regarded as an AMIP-style simulation in which the observed monthly SST and SIC [*Rayner et al*., 2003] were prescribed. A 25 year future global-warmed (GW) projection (2075–2099) was conducted with prescribed future SST, SIC, and atmospheric concentration of greenhouse gases, including CO_2 and aerosols, based on the Intergovernmental Panel on Climate Change (IPCC) Special Report on Emission Scenarios A1B scenario [*Solomon et al*., 2007]. The future changes and trends of SST and SIC were estimated from the ensemble mean of 18 models from the World Climate Research Programme's Coupled Model Inter-comparison Project phase 3 [*Meehl et al*., 2007] under the IPCC A1B scenario, and the future anomalies were superposed onto the detrended observed monthly SST and SIC to construct lower-boundary conditions for the GW projection [*Mizuta et al*., 2008].

2.2. Box Difference Index and Examined Parameters

[5] The domain of interest in this study is the tropical WNP (0–25°N, 100–180°E) and NA (0–25°N, 100°W–10°E). Developing and nondeveloping disturbances were detected according to the criteria of maximum relative vorticity, and other parameters, using 6 hourly outputs (see details in auxiliary material). Once the developing and nondeveloping disturbances were identified, 20 day low-pass filtered fields in a $20^\circ \times 10^\circ$ longitude-latitude box centered on the cyclonic circulation are examined. To identify the differences in various variables for the developing and nondeveloping groups, composites are made using the filtered fields for each day of the 4 day period prior to the cyclogenesis date (designated as day −3, –2, –1, and 0) for the developing disturbances, and every day for all nondeveloping disturbances over their entire lifespan.

[6] The BDI [*Peng et al*., 2012] is used to distinguish the difference of a variable associated with two groups of the developing and nondeveloping disturbances. BDI is defined as follows:

$$BDI = \frac{M_{\mathrm{DEV}} - M_{\mathrm{NONDEV}}}{\sigma_{\mathrm{DEV}} + \sigma_{\mathrm{NONDEV}}},$$

where M and σ respectively represent the composite area mean and its standard deviation of a 20 day low-pass filtered variable in the $20^\circ \times 10^\circ$ box centered at each disturbance. The subscript DEV and NONDEV respectively represents developing and nondeveloping ensemble. A high value of BDI is obtained if the difference in the area mean variable is large between the two groups, and if both groups have a small variance, indicating that the two groups can be clearly distinguished by this variable. Because BDI is a nondimensional parameter, its value can be directly compared among all of the dynamic and thermodynamic variables, so that the relative importance of these large-scale variables in cyclogenesis can be determined. In this study, we only focus on BDI at day −1 because there is a large number of samples from day −1. (A similar result was obtained for the BDI at day −2.) BDI results are also dependent on grid size. Our calculations using different grid sizes of $20^\circ \times 20^\circ$, $20^\circ \times 10^\circ$, and $10^\circ \times 10^\circ$ showed that similar results were obtained with $20^\circ \times 10^\circ$ and $10^\circ \times 10^\circ$ grid boxes, but that their BDI values are in general greater than those obtained using a $20^\circ \times 20^\circ$ grid box. Because we focus on large-scale environmental conditions, a larger grid box with a higher BDI is preferable, so we will focus on the BDI defined using the $20^\circ \times 10^\circ$ grid box throughout this study.

[7] Using the BDI computation, several dynamic variables have identified including relative vorticity at 500 hPa (ξ), divergence at 850 hPa (700 hPa for the NA) (D), vertical pressure-velocity at 250 hPa (ω), and vertical wind shear (VS), and the thermodynamic variables of relative humidity at 700 hPa (RH), precipitation (Pr), and SST. For the variables with multiple vertical levels, we first identified a level with maximum (or nearly maximum) BDI out of all vertical levels available in the outputs, and then took this to be the representative level for the variable. For the same variable, the level changes little between the present-day and future simulations in either basin, indicating that the critical vertical level that separates the two types of disturbances will not vary significantly under a warmer global climate in this study. Therefore, we use a fixed vertical level to compare BDIs for both the present-day simulation and future projection. *Peng et al*. [2012] and *Fu et al*. [2012] found different vertical levels that can best distinguish VS in the two basins. In this study, we found that wind speed differences between 200 and 850 hPa are most appropriate for defining VS in the WNP (200–700 hPa for the NA) based on the composite mean of the vertical profiles of zonal wind around the disturbances (figure not shown).

3. Results and Discussion

3.1. Number of Disturbances

[8] The annual mean counts of observed and simulated/projected developing and nondeveloping disturbances are shown in Table 1. Figure S1 also shows the daily displacement vector of the developing (starting at days −3, –2,

Table 1. Annual Mean Counts of Developing Disturbances From (a) Observations (1979–2003), (b) Present-Day (PD) Simulation (1979–2003), and (c) Future (GW) Projection (2075–2099), and Nondeveloping Disturbances From (d) PD Simulation, and (e) GW Projection Counted in all Seasons (ALL) and Only the June–September (JJAS) Season for Each Western North Pacific (WNP) and North Atlantic (NA)

Season	(a) Observed Developing	(b) PD Developing	(c) GW Developing	(d) PD Nondeveloping	(e) GW Nondeveloping
			Western North Pacific		
ALL	26.5	25.6	18.7	21.2	20.1
JJAS	16.0	14.5	9.5	10.8	10.5
			North Atlantic		
ALL	10.5	7.3	5.5	18.0	16.8
JJAS	8.0	6.4	5.0	11.4	10.1

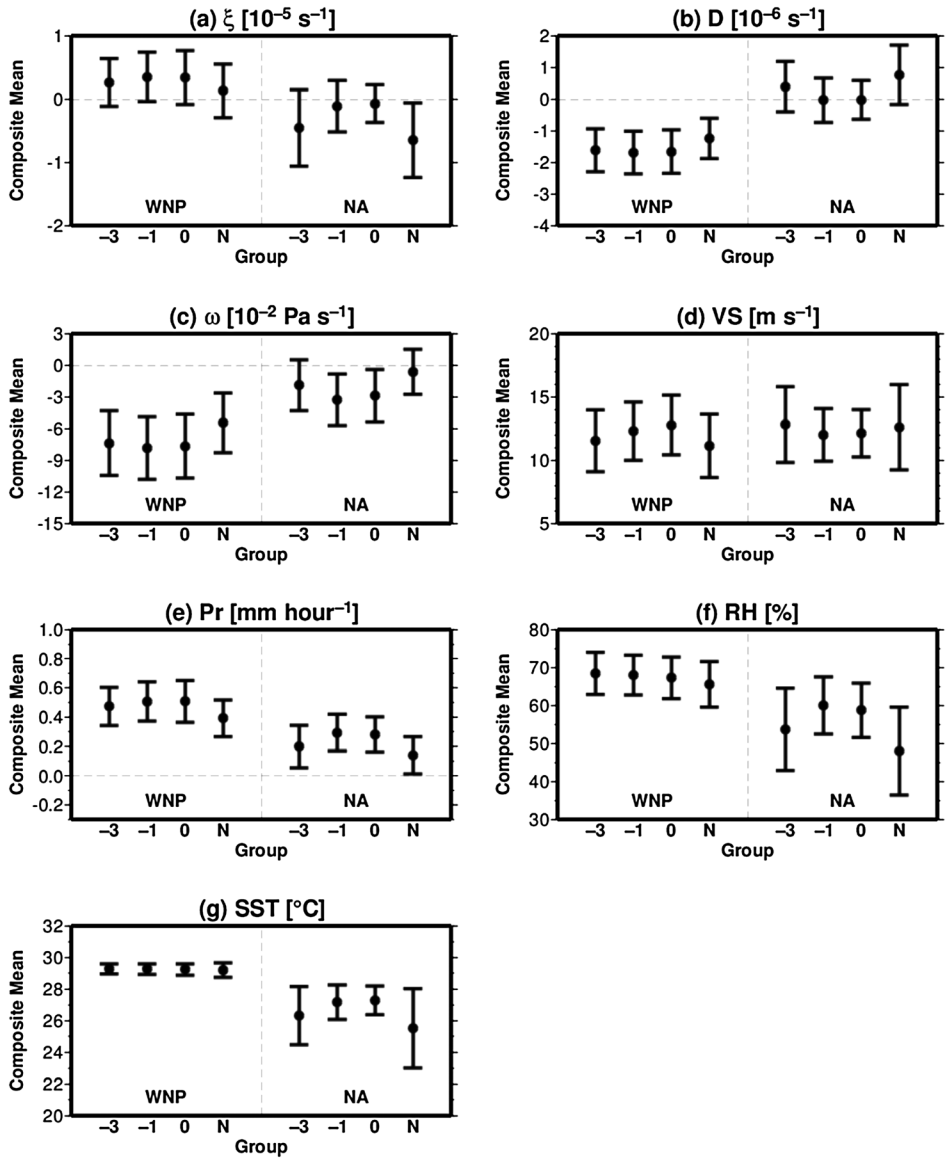

Figure 1. Composite area mean of 20 day filtered variables in a grid box of 20° × 10° during the summer season computed by the PD simulation for (a) relative vorticity at 500 hPa [10^{-5} s^{-1}], (b) low-level divergence at 850 hPa for the WNP and 700 hPa for the NA, (c) vertical pressure-velocity at 250 hPa [10^{-2} Pa s^{-1}], (d) vertical wind shear [m s^{-1}], (e) precipitation [mm h^{-1}], (f) relative humidity at 700 hPa [%], and (g) sea surface temperature [°C]. The error bars indicate one standard deviation. Each panel shows composites at days −3, –1, and 0 prior to cyclogenesis for developing disturbances, and every day for nondeveloping disturbances (N) in the WNP and NA.

and −1) and nondeveloping disturbances (starting at each day of its lifespan). The PD simulation yielded an annual mean number of developing disturbances that is reasonably close to the observed (1979–2003) values (Table 1), although the simulated number of developing disturbances for the NA is a little low. As documented by *Murakami et al*. [2012a], a statistically significant decrease in the number of developing disturbances is projected for GW period (at the 99% level by Welch's *t*-test) in both basins especially in the summer season of June–September; therefore, this study mainly focuses on the summer season. The number of nondeveloping disturbances in the PD simulation is less than the number of developing disturbances in the WNP, whereas it is about two- or three-times larger in the NA. The projected future change in the number of nondeveloping disturbances is not statistically significant in either basin.

3.2. Composite Mean

[9] To assess the differences in large-scale background conditions between the developing and nondeveloping groups, Figure 1 shows composite mean and variance of 20 day filtered variables in a 20° × 10° grid box centered on each disturbance during the summer season obtained by the PD simulation. Figure S2 also shows their counterparts in the GW projection. For the midlevel vorticity (ξ) at 500 hPa (Figure 1a) and low-level divergence (Figure 1b), there are distinct differences between the developing and nondeveloping groups, indicating that these dynamic factors are critical factors in the separation of the two groups. Note

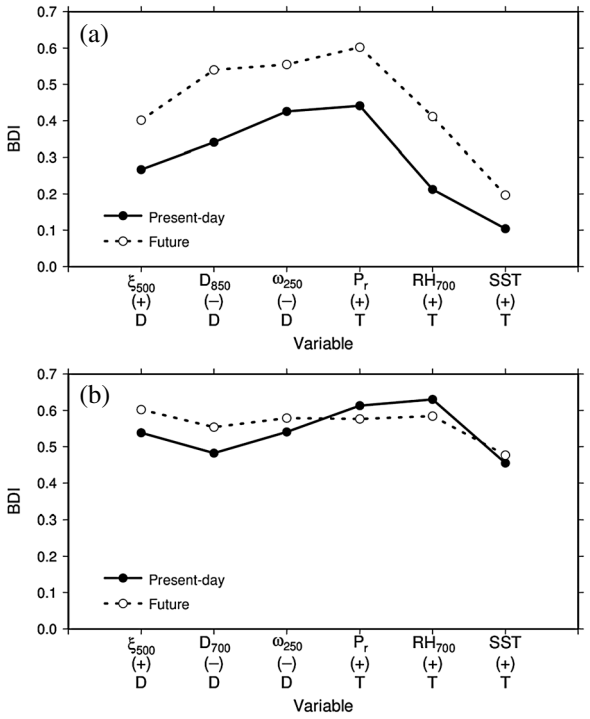

Figure 2. BDI values associated with the different large-scale variables for (a) the WNP and (b) the NA. Solid lines are BDIs for present-day simulation, while dotted lines are BDIs for future projection. Parentheses indicate the sign of the BDI for the variable. *D* denotes a dynamic variable, while *T* denotes a thermodynamic variable.

that mean variables in two groups in the NA are opposite in sign to those in the WNP: anticyclonic background flow at 500 hPa and low-level divergence at 700 hPa are not favorable for the development of TCs in the NA. Mean vertical pressure-velocity (ω) with a negative sign (i.e., upward motion) at 250 hPa (Figure 1c) and precipitation (*Pr*) (Figure 1e) are also markedly larger in the developing groups than in the nondeveloping group in both basins, indicating that background deep convection is one of the critical factors that separate the two groups. Vertical wind shear (*VS*) (Figure 1d) shows an interesting feature: mean shear is larger in the developing groups than in the nondeveloping group in the WNP, which is consistent with observations [*Fu et al*., 2012], indicating that the background vertical wind shear does not have a critical role in cyclogenesis in the WNP. For the relative humidity (*RH*) at 700 hPa (Figure 1f), both basins show higher values in the developing groups than in the nondeveloping group. As for SST (Figure 1g), the mean differences between the developing and nondeveloping groups are larger in the NA than in the WNP as this basin contrast is also seen in *RH*.

3.3. BDI, its Future Change, and the Implications

[10] To assess the relative importance of the controlling environmental variables, and to investigate possible future changes under global warming, Figure 2 shows the BDI related to the key large-scale variables in each basin for both the present-day and future climate simulations. In the figure, we ruled out *VS* because it shows smaller BDI compared with other variables in both basins.

[11] In the WNP (Figure 2a) under the present-day climate (solid line), the BDIs associated with the dynamic variables (e.g., ξ, *D*, and ω) are larger than those for the thermodynamic variables (except for *Pr*), which indicates that the dynamic variables are of primary importance in the separation of the developing and nondeveloping groups. Although the order of the top BDI parameters does not change in the future projection (dotted line in Figure 2a), marked increases in the BDI values can be seen for all variables. These results suggest that it will be easier to separate developing and nondeveloping disturbances in a warmer climate state; as a result, potential future TC genesis in the WNP will be more predictable.

[12] In the NA (Figure 2b), the BDIs computed with the PD simulation are greater for the thermodynamic variables (e.g., *Pr* and *RH*) than for the dynamic variables (e.g., ξ, *D*, and ω) except for SST. Moreover, the BDIs of the thermodynamic variables (e.g., *RH* and SST) are greater than their WNP counterparts. These results indicate that thermodynamic variables are more important in the separation of the developing and nondeveloping groups in the NA under the present-day climate, which is consistent with observational studies [*Peng et al*., 2012; *Fu et al*., 2012]. Although future changes in BDIs are smaller than those in the WNP, every dynamic variable shows an increase in BDI, while most of the thermodynamic variables show either a decrease, or little change. This indicates that dynamic and thermodynamic variables become equally important in the NA under a future warmer climate state.

[13] The systematic increases in BDIs in the WNP were mostly due to the increases in the mean value of the variables in the developing groups, indicating that necessary background conditions for TC genesis become stricter in the warmer climate than in the present-day climate. The reason for the stricter necessary conditions may be due to the changes in the climatological mean vertical structures of temperature and mass flux in tropics. Figure 3 shows projected future changes in JJAS mean static stability, upward motion at 500 hPa, low-level specific humidity at 850 hPa, and SST in the main develop regions (10°N–20°N, 110°E–160°E for WNP; 7.5°N–17.5°N, 20°W–40°W for NA). In the WNP, although low-level moisture and SST are projected to increase in the future, marked increase in static stability and reduction in the upward motion can be seen, which may lead to inactive convection in the tropics and result in less convection to aggregate and develop into a TC.

[14] In contrast, in the NA, the increases in BDI for the dynamic variables were mostly due to relatively larger decreases in the mean value of the nondeveloping group rather than the increases in the mean value of the developing groups, indicating that in the future, two groups are more distinguishable by the dynamic variables compared with the present-day climate state. In contrast to the WNP, mean upward motion is projected to slightly increase in the future in the main develop region in the NA. Moreover, in the NA, climatological mean thermodynamic variables, such as low-level moisture and SST become closer to those of the WNP present-day climate. These results suggest that in the future the controlling mechanism for TC genesis in the NA might resemble more like that in the current WNP climate state.

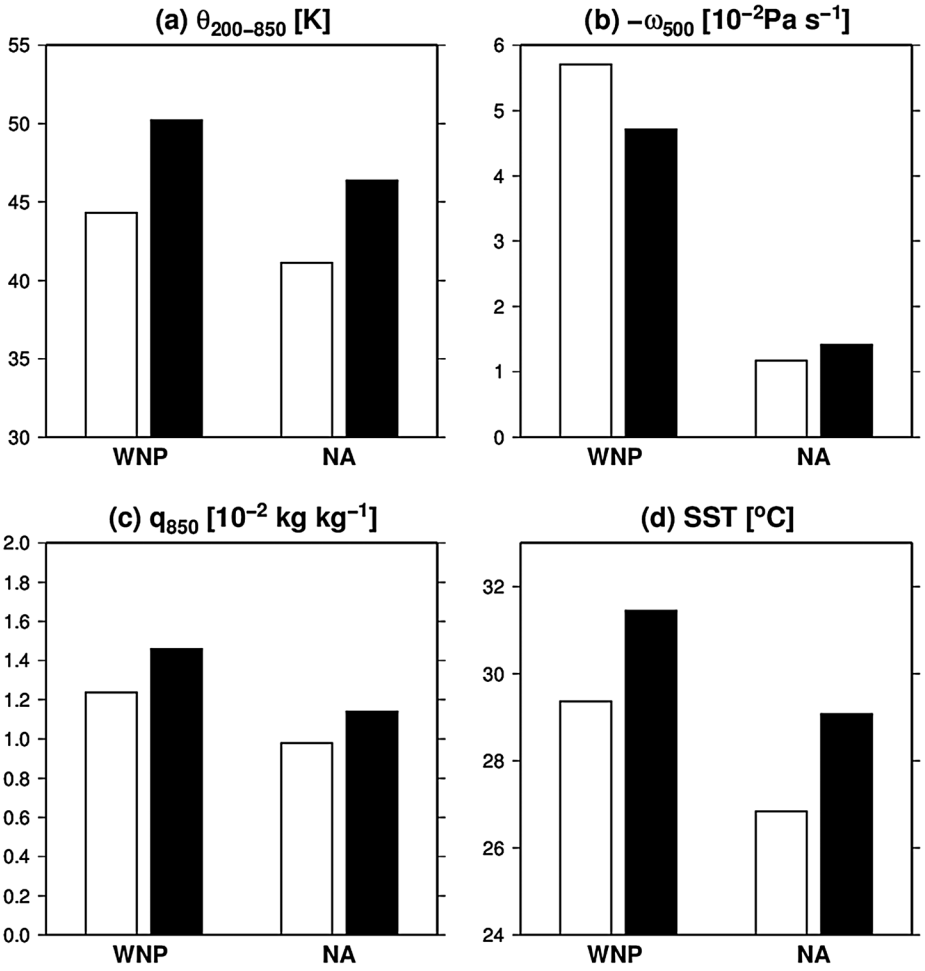

Figure 3. Area mean of climatological mean variables during the summer season over the main develop regions (10°N–20°N, 110°E–160°E for the WNP; 7.5°N–17.5°N, 20°W–40°W for the NA) for (a) static stability [K] (defined as the difference in potential temperature between 200 and 850 hPa), (b) vertical upward *p*-velocity at 500 hPa [10^{-2} Pa s^{-1}], (c) specific humidity at 850 hPa [10^{-2} kg kg^{-1}], and (d) SST [°C]. White (Black) bars indicate mean value by the present-day simulation (future projection).

4. Summary

[15] The objective of this study is to investigate if global warming will change the large-scale controlling parameters for TC genesis. A BDI was computed to diagnose the PD simulation (1979–2003) and GW projection (2075–2099) under the IPCC A1B scenario conducted by a 20 km resolution global climate model (MRI-AGCM3.2). The targeted ocean basins were the tropical WNP and the NA.

[16] The annual mean count of developing disturbances is well simulated by the model for the PD period. In the GW projection period, the number of developing disturbances is projected to decrease significantly in both basins, while the projected number of nondeveloping disturbances has little change.

[17] The BDI analysis in the PD simulation revealed that dynamic variables are of primary importance for separating developing and nondeveloping disturbances in the WNP, while thermodynamic variables are of primary importance in the NA. These results were consistent with the observational studies of *Peng et al.* [2012] and *Fu et al.* [2012].

[18] Under global warming climate, BDIs in the WNP increase for all the dynamic and thermodynamic variables investigated. The increases are primarily attributed to the increase of the mean values in the developing groups. Because of the greater BDI values, it becomes easier to separate developing and nondeveloping groups in a warmer climate. Thus, cyclogenesis forecast will be easier in the future. In contrast, in the NA, while the BDIs for dynamic variables increase, most of thermodynamic variables show either a decrease in BDI or little change. As a result, the dynamic and thermodynamic variables have about equal control in the NA under a future warmer climate.

[19] Overall, we conclude that large-scale environmental variables that control TC genesis will change under a warmer future climate: more favorable background conditions are required for TC genesis event in the WNP, while dynamic variables become more important compared with the present-day climate in the NA. These results indicate that one may not use the same GPI formula globally to identify future changes in TC genesis frequency. A further study to apply the BDI methodology to other models is needed to determine whether the conclusions reached here are model-dependent. It may be worthwhile constructing a GPI formula for each basin, to develop a better understanding of the environmental factors that control the

interannual variation of TC genesis frequency in each basin.

[20] **Acknowledgments.** This work was supported by ONR grant N000141210450, by the "KAKUSHIN" and "SOUSEI" programs of the University of Tsukuba, and by the International Pacific Research Center (IPRC) that is sponsored by the JAMSTEC, NASA and NOAA. High-resolution model simulations were performed on the Earth Simulator. This contribution is School of Ocean and Earth Science and Technology publication No. 8907 and International Pacific Research Center publication No. 970.

[21] The Editor thanks 2 anonymous reviewers for their assistance in evaluating this paper.

References

Bengtsson, L., M. Botzet, and M. Esch (1996), Will greenhouse gas-induced warming over the next 50 years lead to higher frequency and greater intensity of hurricanes?, *Tellus*, *48A*, 57–73, doi:10.1034/j.1600-0870.1996.00004.X.

Emanuel, K. A., and D. S. Nolan (2004), Tropical cyclone activity and global climate. Preprints, *26th Conf. on Hurricanes and Tropical Meteorology*, Miami, FL, Amer. Meteor. Soc., 240–241.

Fu, B., M. S. Peng, and T. Li (2012), Developing versus nondeveloping disturbances for tropical cyclone formation. Part II: Western North Pacific, *Mon. Wea. Rev.*, *140*, 1067–1080, doi:10.1175/2011MWR3618.1.

Knutson, T., et al. (2010), Tropical cyclones and climate change. *Nat. Geosci.*, *3*, 157–163, doi:10.1038/ngeo779.

Lavender S. L., and K. J. E. Walsh (2011), Dynamically downscaled simulations of Australian region tropical cyclones in current and future climate, *Geophys. Res. Lett.*, *38*, L10705, doi:10.1029/2011GL047499.

Li, T. (2012), *Synoptic and climatic aspects of tropical cyclogenesis in Western North Pacific*, edited by K. Oouchi and H. Fudeyasu, Chap.3, pp. 61–94, Nova Science Publishers, Inc. New York.

Li, T., M. Kwon, M. Zhao, J. Kug, J. Luo, and W. Yu (2010), Global warming shifts Pacific tropical cyclone location, *Geophys. Res. Lett.*, *37*, L21804, doi:10.1029/2010GL045124.

Meehl, G., C. Covey, T. Delworth, M. Latif, B. McAvaney, J. Mitchell, R. Stouffer, and K. Taylor (2007), The WCRP CMIP3 multi-model dataset: A new era in climate change research, *Bull. Am. Meteorol. Soc.*, *88*, 1383–1384, doi:10.1175/BAMS-88-9-1383.

Mizuta, R., Y. Adachi, S. Yukimoto, and S. Kusunoki (2008), Estimation of the future distribution of sea surface temperature and sea ice using the CMIP3 multi-model ensemble mean, *Tech. Rep. Meteor. Res. Inst.*, *56*, 34.

Mizuta, R., et al. (2012), Climate simulations using MRI-AGCM3.2 with 20-km grid, *J. Meteor. Soc. Japan*, *90A*, 233–258, doi:10.2151/jmsj.2012-A12.

Murakami, H., B. Wang, and A. Kitoh (2011), Future change of western North Pacific typhoons: Projections by a 20-km-mesh global atmospheric model, *J. Clim.*, *24*, 1154–1169, doi:10.1175/2010JCLI3723.1.

Murakami, H., et al. (2012a), Future changes in tropical cyclone activity projected by the new high-resolution MRI-AGCM, *J. Clim.*, *25*, 3237–3260, doi:10.1175/JCLI-D-11-00415.1.

Murakami, H., R. Mizuta, and E. Shindo (2012b), Future changes in tropical cyclone activity projected by multi-physics and multi-SST ensemble experiments using the 60-km-mesh MRI-AGCM, *Clim. Dyn. 39*, 2569–2584, doi:10.1007/s00382-011-1223-X.

Nolan, D. S., and E. D. Rappin (2008), Increased sensitivity of tropical cyclogenesis to wind shear in higher SST environments, *Geophys. Res. Lett.*, *35*, L14805, doi:10.1029/2008GL034147.

Peng, M. S., B. Fu, and T. Li (2012), Developing versus nondeveloping disturbances for tropical cyclone formation. Part I; North Atlantic, *Mon. Wea. Rev.*, *140*, 3, doi:10.1175/2011MWR3617.1.

Rayner, N. A., D. E. Parker, E. B. Horton, C. K. Folland, L. V. Alexander, and D. P. Rowell (2003), Global analysis of sea surface temperature, sea ice, and night marine air temperature since the late nineteenth century, *J. Geophys. Res.*, *108*(2494), 4407, doi:10.1029/2002JD002670.

Solomon, S., D. Qin, M. Manning, M. Marquis, K. Averyt, M. M. B. Tignor, H. L. Miller Jr., and Z. Chen Eds. (2007), Climate Change 2007: *The Physical Science Basis*. Cambridge University Press, 996 pp.

Vecchi, G. A., and B. J. Soden (2007), Increased tropical Atlantic wind shear in model projections of global warming, *Geophys. Res. Lett.*, *34*, L08702, doi:10.1029/2006GL028905.

Yokoi, S., and Y. N. Takayabu (2009), Multi-model projection of global warming impact on tropical cyclone genesis frequency over the western North Pacific, *J. Meteor. Soc. Japan*, *87*, 525–538, doi:10.2151/jmsj.87.525.

Zhao, M., and I. M. Held (2012), TC-permitting GCM simulations of hurricane frequency response to sea surface temperature anomalies projected for the late 21st century, *J. Clim.*, *25*, 2995–3009, doi:10.1175/JCLI-D-11-00313.1.